cea iresne

Resolving multi-scale two-phase flows in mini-channels

Optical measurements and interface tracking

Dr. Jimmy MARTIN

GDR TransInter – Journées d'Aussois 2026

April 7, 2026

1. Capillary-dominated flows: context and challenges

Compact heat exchangers for advanced energy systems

- **Compact heat exchangers** are a key technology for advanced energy systems, including **Small Modular Reactors (SMRs)**.
- They rely on **dense arrays of millimeter-scale channels** providing **very high surface-to-volume ratios** and **enhanced heat transfer**.
- Recent developments combine **diffusion-bonded metallic plate heat exchangers** and **additively manufactured architectures** with complex 3-D flow pathways.

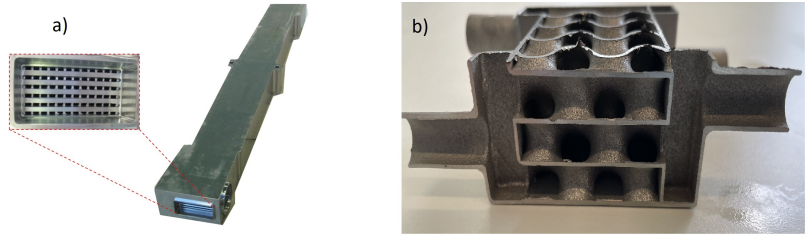

Examples of compact heat exchanger technologies investigated at CEA: (a) diffusion-bonded stainless-steel mini-channel heat exchanger; (b) additively manufactured heat exchanger based on a TPMS architecture.

Two-phase flows in millimeter-scale channels

- In compact heat exchangers, gas–liquid flows develop in **millimeter-scale channels**, typically ranging from **200 µm to a few millimeters**.
- These flows operate in an **intermediate regime** between **microfluidics (creeping flows)** and classical **macro-scale turbulent flows**.
- At these scales, **capillary effects become significant** while **gravitational effects tend to be comparatively weaker**.
- Under such **strong confinement**, the interaction between the fluid and the **channel wall** becomes a controlling factor.

Research gap

Most experimental studies of two-phase flow regimes in mini-channels rely on transparent materials (Pyrex, polymers) enabling direct flow visualization. However, industrial thermal systems are manufactured from metallic materials (stainless steels, nickel alloys, titanium), for which **quantitative hydrodynamic data remain scarce**. This lack of data partly **limits the development and validation of compact thermal systems**.

Experimental challenges

Heat exchangers are typically made of **opaque metallic materials**: **direct flow visualization** is therefore **not possible** in such components.

Alternative diagnostic techniques for opaque materials

Possible approaches rely on **large-scale radiographic facilities**, allowing either **neutron or synchrotron X-ray imaging**.

The European Synchrotron Radiation Facility (ESRF) in Grenoble (© J. CHAVY).

A proposed optical time-of-flight method

Proposed methodology

In this study, we revisit an **optical probe technique** originally developed for local void fraction measurements in macro-channel two-phase flows and adapt it to **millimeter-scale confined flows**. Two axially separated optical probes are used to:

- Detect the **local phase indicator function**.
- Measure the **time-of-flight of gas structures**.
- Reconstruct the **propagation velocity** and **axial chord lengths** of gas structures.

Investigated system

The methodology is applied to adiabatic **air–water flows** in a **4 mm inner-diameter stainless steel mini-channel (316L)**, with an **axial probe spacing of $\sim$110 mm**.
Two distinct flow regimes are reproduced on the **BICHE experimental loop (CEA/IRESNE)**: **Taylor-bubble flow** and **intermittent–annular transition flow**.

2. BICHE test device and its instrumentation

The BICHE experimental loop at CEA/IRESNE

- **BICHE** is an analytical experimental device developed at CEA/IRESNE to **investigate capillary-dominated two-phase flows in millimetric channels**.
- The loop reproduces **two-phase hydrodynamic conditions encountered in compact steam generators**.
- The loop is equipped with two independent hydraulic circuits, each fitted with a volumetric circulation pump, allowing a liquid mass flow rate range from **0.3 to 200 g/s**.
- A compressed gas injection line is installed upstream of each test section.
- The loop operates in a pressure range between **1 and 10 bar**.

BICHE piping and instrumentation diagram

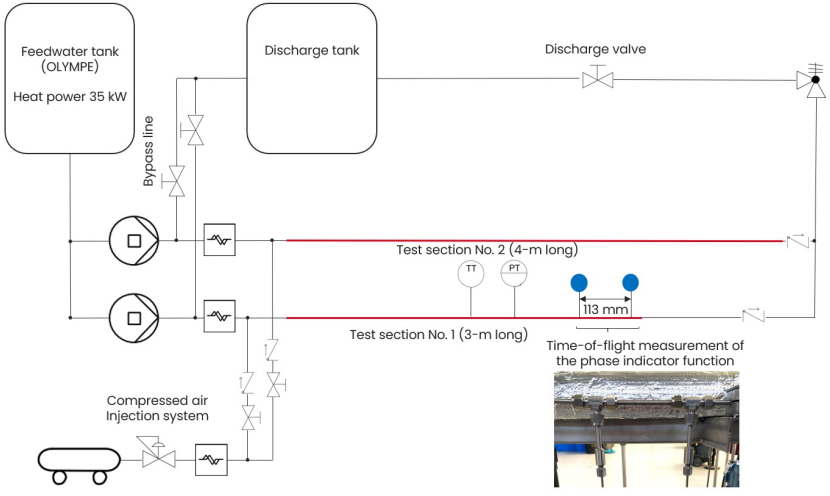

Process instrumentation and data acquisition system

- The operating conditions of the BICHE loop are monitored through a dedicated process instrumentation.
- Liquid and injected air mass flow rates are measured using high-precision Coriolis flow-meters.
- Temperature and absolute pressure are continuously monitored along the loop.
- All process measurements are recorded using a National Instruments data acquisition system at a sampling frequency of **1 Hz**.

Process instrumentation used for monitoring the operating conditions of the BICHE loop

Measurement	Sensor	Range	Precision (k=2)
Liquid mass flow rate	Coriolis flow-meter, Elite series (MICROMOTION)	0 – 200 g/s	$\pm$0.1 % measurement
Injected air mass flow rate	Coriolis flow-meter, Elite series (MICROMOTION)	0 – 5 g/s	$\pm$0.1 % measurement
Temperature	Pt-100 1/10^{e} DIN probe	0 – 100°C	$\pm$0.15 K
Absolute pressure	Pressure transducer EMERSON 3051	0 – 10 bar	$\pm$0.2 % measurement

Optical phase detection

- Local phase detection is performed using **RBI optical probes** inserted transversely to the flow through **Swagelok T-fittings**.
- Each probe consists of a **sharpened fused-silica optical fiber** (tip diameter $\approx 60\,\mu$m) housed in a stainless-steel support.

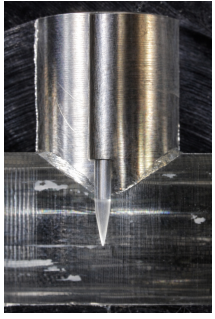

Fused-silica probe tip positioned at the channel centerline.

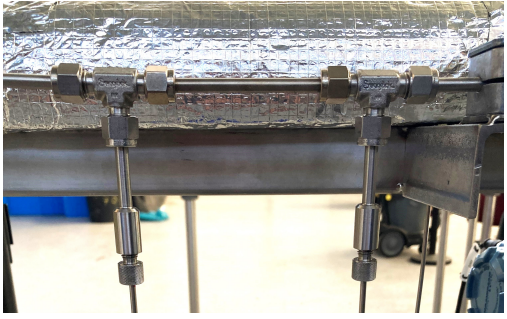

Dual optical probe configuration for time-of-flight measurements ($L \approx 110$ mm).

Optical phase detection

- The **measurement principle relies on the difference in refractive index between the gas and liquid phases**:
  - When the sensing tip is **exposed to liquid**, the emitted light refracts into the liquid, producing a **low reflected optical signal**;
  - When the sensing tip is **exposed to gas**, the light is mostly reflected back into the fiber, generating a **strong return signal**.
- The returned light intensity is detected by an optical-electronic device. The presence or absence of detected photons is converted into an analogue voltage signal in the range **0–10 V**.

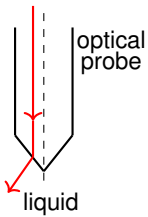

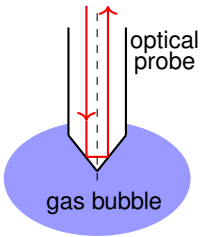

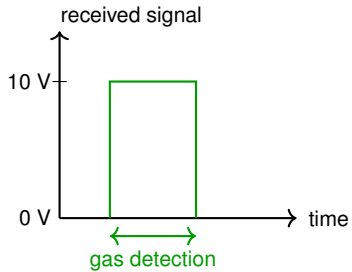

3. An interface tracking optical method

Description of the interface tracking optical method

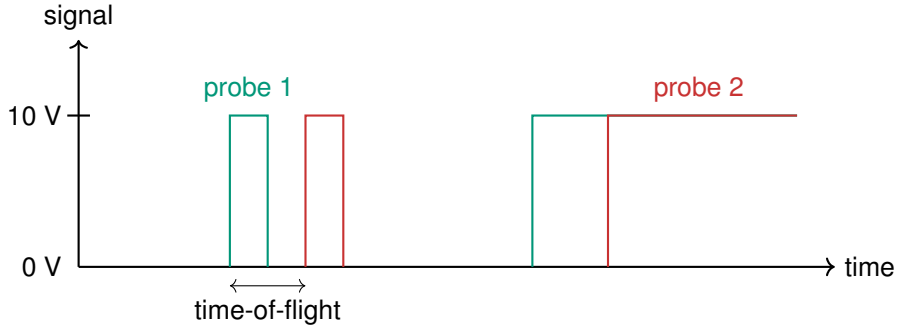

- **Two optical probes** are installed along the channel centerline. The axial distance between sensing tips is denoted as L.
- **Gas–liquid interfaces successively intersect** the **upstream** and **downstream probes**.
- The propagation of each detected interface is reconstructed through a **deterministic front-tracking procedure**.

Description of the interface tracking optical method

1. **Voltage acquisition:** Each optical probe delivers a continuous voltage signal $V_i(t)$ reflecting the phase present at the sensing tip.
2. **Phase indicator construction:** The analogue signal is converted into a binary phase indicator $\chi_i(t)$ using a fixed detection threshold.
3. **Interface detection:** Gas–liquid interfaces are identified as discontinuities of the phase indicator signal.
4. **Noise filtering:** Short events caused by optical spikes are removed using a minimum duration criterion.
5. **Deterministic front matching:** Interfaces detected at the upstream probe are associated with those detected at the downstream probe using physically admissible propagation delays.
6. **Velocity reconstruction:** The interface velocity is obtained from the time-of-flight between probes.
7. **Chord reconstruction:** Gas chord lengths are determined from the residence time of the gas phase at the probe.

Phase indicator construction

The **analogue voltage signal** associated with each probe is **converted into a binary phase indicator**, denoted as $\chi_i(t)$, with $i = 1, 2$ refering respectively to the upstream and downstream probes:

$$\chi_i(t) = \begin{cases} 1 & \text{if gas is detected} \\ 0 & \text{if liquid is detected} \end{cases}$$

Using a fixed detection threshold V_{th}, this yields:

$$\chi_i(t) = 1 - \mathcal{H}\left(V_i(t) - V_{th}\right)$$

with $\mathcal{H}(\cdot)$ denoting the *Heaviside* function and $V_{th} = 6$ V.

Why binarizing the signal?

The raw voltage signal is not perfectly 0–10 V: it may contain **noise**, **offset**, and **amplitude fluctuations**. The binary phase indicator provides a **robust phase detection** independent of these variations.

Interface detection

Gas–liquid interfaces correspond to **discontinuities of the phase indicator signal**. In this framework, a gas front arrival is defined by:

$$\frac{d\chi_i}{dt} > 0$$

In discrete form, interface detection reduces to evaluating the signal increment:

$$\Delta\chi_i(k) = \chi_i(k+1) - \chi_i(k)$$

Interface identification

The applied rule:

$$\begin{cases} \Delta\chi_i = +1 & \text{corresponds to gas front interface} \\ \Delta\chi_i = -1 & \text{corresponds to gas rear interface} \end{cases}$$

Interface detection therefore reduces to detecting **transitions in the binary phase signal**.

Noise filtering

Optical probe signals may contain **short spurious events** caused by optical noise or interface fluctuations. These unwanted events are removed using a **minimum duration criterion**.

Filtering criterion

An event is discarded if its duration satisfies:

$$n_{event} < n_{min}$$

with:

$$n_{min} = 3 \text{ samples}$$

Since the sampling interval is Δt, the minimum physical duration retained is

$$t_{min} = 3\,\Delta t$$

This procedure removes short optical spikes while preserving physical gas structures.

Deterministic front matching

The propagation of each gas–liquid interface between the two probes is reconstructed by associating detections corresponding to the **same physical interface**. Let:

$$t_{1,k}, \qquad t_{2,j}$$

be the arrival times of gas fronts detected at probes 1 and 2.

- k indexes gas fronts detected at the **upstream probe**.
- j indexes gas fronts detected at the **downstream probe**.
- Each detected interface therefore generates two arrival times, one at each probe.

The signal propagation delay between the probes τ – or **time-of-flight** – is:

$$\tau = t_{2,j} - t_{1,k}$$

Deterministic front matching

In practice, several interfaces may be present simultaneously in the probe signals. A matching criterion is therefore required to **avoid incorrect associations**.

Matching criterion

Interface propagation velocities must satisfy:

$$U_{min} \leq \frac{L}{\tau} \leq U_{max}$$

with:

$$U_{min} = 0.05 \text{ m s}^{-1}, \qquad U_{max} = 15 \text{ m s}^{-1}$$

These bounds correspond to the **envelope of superficial velocities** achievable in the experimental facility.

- If τ is too small $\rightarrow$ unrealistically high velocity.
- If τ is too large $\rightarrow$ the detections likely correspond to different interfaces.

Interface velocity reconstruction

Once a pair of fronts has been successfully matched, the interface propagation velocity can be determined from the measured **time-of-flight** τ.

Hence, the interface velocity U_k associated with event k is:

$$U_k = \frac{L}{\tau_k}$$

where:

- L is the axial distance between the two probes.
- τ_k is the measured delay between the two detections occurring during event k.

Each matched interface therefore provides one instantaneous estimate of the **interface velocity**.

Gas chord reconstruction

The axial length of each detected gas structure is reconstructed from the **residence time of the gas phase** at the probe. Let:

$$\Delta t_k = t_{b,k} - t_{f,k}$$

be the gas residence time measured at probe 1, where

- $t_{f,k}$ is the **gas front arrival**
- $t_{b,k}$ is the **rear interface detection**

The corresponding gas chord length is:

$$\ell_k = U_k \Delta t_k$$

Each detected gas structure therefore provides a pair:

$$(U_k, \ell_k)$$

used to **build statistical distributions of interface velocities and gas chord lengths**.

4. Experimental results and discussion

The generated experimental database

A systematic experimental campaign was conducted to evaluate the capability of an **interface tracking optical method** to resolve gas–liquid flow structures in confined mini-channels

Experimental conditions

- **68 explored operating conditions**
- **Achieved mass fluxes:**

$$60 \leq G \leq 380 \text{ kg.m}^{-2}.\text{s}^{-1}$$

- **Reached Reynolds numbers:**

$$190 \leq Re_L \leq 1400 \qquad 220 \leq Re_G \leq 2600$$

- **Acquisition time:** 60 s
- **Sampling frequency:**

$$f_s = 125 \text{ kHz} \qquad (\Delta t = 8\,\mu s)$$

Achieved two-phase flow regimes

The explored operating conditions were interpreted using the **generalized flow regime map proposed by *Shin and Kim* in 2022, for mini- and micro-channels**.

- The **full experimental database** is represented by **yellow markers**.
- Most operating conditions lie within the so-called **intermittent** and **transition** regions.
- Two representative groups of operating points were selected for detailed analysis: These points correspond to the most contrasted **gas-phase organisations** observed in the present study (red and blue markers).

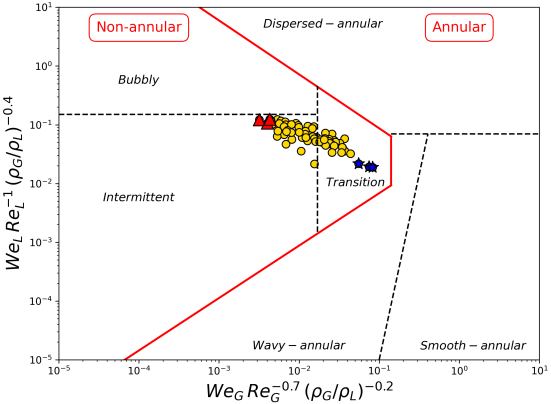

Flow regimes investigated in the present study

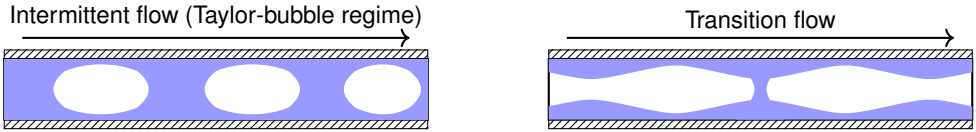

Schematic representation of the **intermittent (Taylor-bubble)** and **transition** flow regimes according to the flow regime map proposed by *Shin and Kim* (2022).

Expected hydrodynamic signatures

- **Taylor-bubble regime:**
  - **Confined bubbles** separated by substantial liquid slugs.
  - **Narrow interface velocity distributions**.
- **Transition regime:**
  - Increasing axial connectivity of the gas phase: **longer gas segments**.
  - **Larger velocity variability** due to interfacial waves.

Hydrodynamic signatures from local statistics

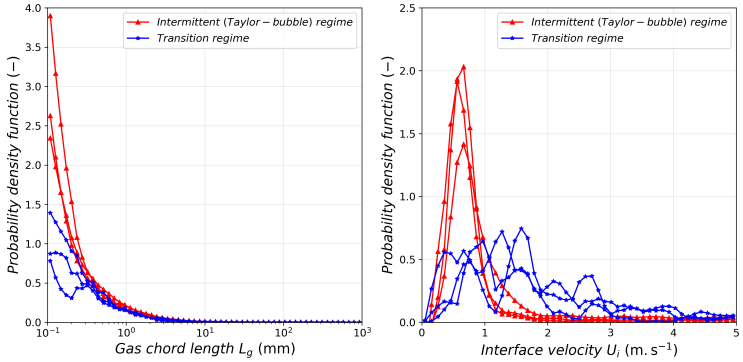

Limited regime discrimination from gas chord length PDFs

- Gas chord length PDFs are **dominated by small gas structures**.
- **Large gas structures remain poorly visible** in gas chord length PDF tails.

Hydrodynamic signatures from local statistics

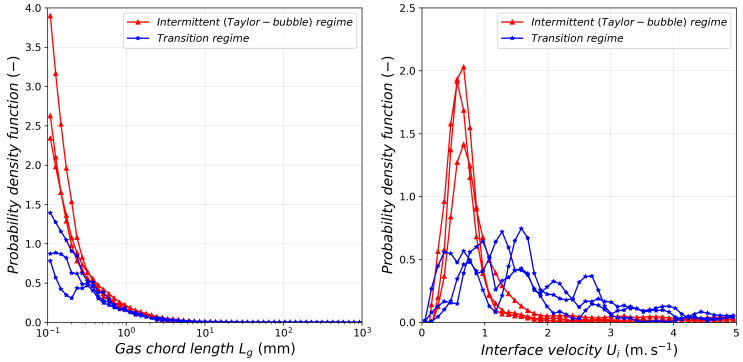

Possible regime discrimination from interfacial velocity PDFs

- Intermittent regime: **narrow velocity distribution**, as expected.
- Transition regime: **broader velocity spectrum**, as expected.

A multi-scale organisation of the gas phase highlighted

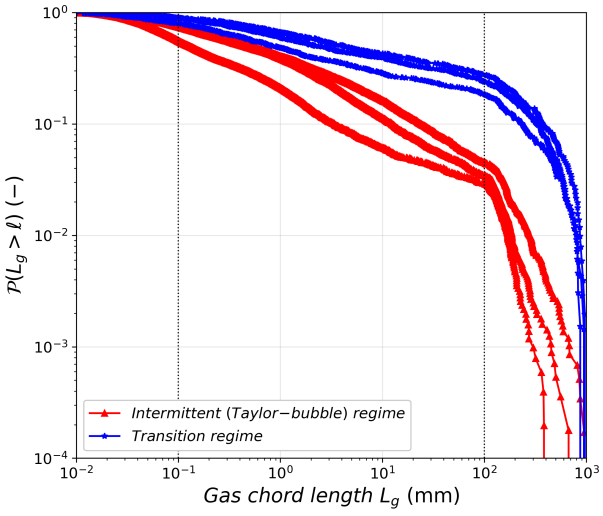

CCDF of gas chord lengths reveal the transition regime

- The CCDF reveals a **multi-scale organisation** of the gas phase spanning several decades of chord length.
- Small scales correspond to **interfacial structures and micro-bubbles**.
- Intermediate scales correspond to **gas pockets and elongated bubbles**.
- The **transition regime exhibits a higher probability of large gas chords**.

5. Conclusions & future work

Conclusions & future work

- A **time-of-flight optical probe methodology** was implemented to resolve the hydrodynamics of gas–liquid flows in a **4 mm stainless-steel mini-channel**.
- The dual-probe measurements provide simultaneous access to **gas chord lengths** and **interface propagation velocities**, enabling a statistical description of the gas-phase organisation.
- **Probability density functions (PDFs)** mainly reflect the most frequent **small-scale gas structures** and provide limited discrimination between flow regimes.
- In contrast, the **complementary cumulative distribution functions (CCDFs)** reveal a clear **multi-scale organisation of the gas phase** and allow a **robust discrimination between intermittent and transition regimes** through the statistics of large gas structures.

Future work

- Extend the statistical analysis to **additional regimes** (bubbly, churn and annular flows).
- Quantify the **scaling laws of CCDF distributions** and relate them to relevant **dimensionless groups**.
- Apply the methodology to **industrial metallic mini-channels** where direct optical visualization is not possible.

iresne

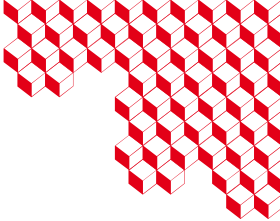

Thank you for your attention

CEA Cadarache Center
F-13115 Saint-Paul-lez-Durance
France
jimmy.martin@cea.fr